MICROPET DETECTION OF 5-HT$_{1A}$ AUTORECEPTOR BINDING IN THE NUCLEUS RAPHE DORSALIS OF RAT USING [^{18}F]MPPF AS RADIOLIGAND

Mélissa LÉVESQUE, BSc

110133102

Graduate Program in Neurological Sciences

McGill University, Montréal, QC

Supervised by

Chawki BENKELFAT, MD, DERBH

and

Laurent DESCARRIES, MD

December 2009

A thesis submitted to McGill University in partial fulfillment of the requirements of the Master's degree.

TABLE OF CONTENTS

ABBREVIATIONS

5,7-DHT: 5,7-dihydroxytryptamine

5-HIAA: 5-hydroxyindoleacetic acid (5-HIAA)

5-HT: 5-hydroxytryptamine; serotonin

5-HT_{1A}R: 5-HT1A receptor

5-HT_{1A}autoR: 5-HT1A autoreceptor

5-HTT: 5-HT transporter

8-OH-DPAT: 8-hydroxy-*N*,*N*-dipropyl-2-aminotetralin

ACh: acetylcholine

AP-2: adaptor protein 2

BP: binding potential

BP_F: binding potential specifically referring to free plasma concentration

BP_{ND}: binding potential specifically referring to nondisplaceable uptake

CNS: central nervous system

DRN: dorsal raphe nucleus

B_2AR: B_2 adrenergic receptor

CXCR4: chemokine (C-X-C motif) receptor 4

FOV: field of view

FWHM: full width half maximum

GABA: γ-aminobutyric acid

GDP: guanine diphosphate

GPCR: G protein coupled receptor

GRK: G protein coupled receptor kinase

GTP: guanine triphosphate

HPA: hypothalamic-pituitary-adrenocortical [system]

i.p.: intraperitoneally

microPET: small animal PET

MNI: Montreal neurological institute

MPPF: 4-(2'-methoxyphenyl)-1-[2'-[N-2"-pyridinyl)-*p*-[(^{18})F]fluorobenzamido]ethyl] piperazine

MRI: magnetic resonance imaging

MRN: medial raphe nucleus

mRNA: messenger ribonucleic acid

NRD: noyau raphé dorsalis

PAR1: protease activated receptor 1

PB: phosphate buffer

PFA: paraformaldehyde

PET: positron emission tomography

PSF: point spread function

ROI: region of interest

SEM: standard error of the mean

SRTM: simplified reference tissue model

SSRI: selective serotonin reuptake inhibitor

V_2R: vasopressin receptor

VOI: voxel of interest

WAY 100635: *N*-(2-(1-(4-(2-Methoxyphenyl)-piperazinyl)ethyl)-*N*-pyridinyl)cyclohexanecarboxamide

ABSTRACT

Abnormal serotonin (5-HT) neurotransmission has been associated with different psychopathologies. Faulty mechanisms that underlie abnormal 5-HT function may include the internalization of the 5-HT_{1A} receptor, located on dorsal raphe nucleus (DRN) serotonin neurons (autoreceptors) and non-serotonin neurons in areas of projection such as hippocampus (heteroreceptors). Upon activation, the 5-HT_{1A} autoreceptor is internalized, a process demonstrated in rat using immuno-electron microscopy. In the current study, we assessed whether labeling of [^{18}F]MPPF, a selective 5-HT_{1A} receptor antagonist, could be detected and measured using microPET in the DRN of rat following fluoxetine mediated internalization of the 5-HT_{1A} autoreceptor. Although internalization was demonstrated in a subsample of rats using immuno-electron microscopy, microPET did not allow for detection of the expected 35% decrease in 5-HT_{1A} autoreceptor labeling in DRN following fluoxetine administration. We propose that the resolution of the microPET scanner, in combination with the anatomical size of the rat DRN, does not permit detection of internalization.

La neurotransmission anormale de la sérotonine (5-HT) a été associée à différentes psychopathologies. Différents mécanismes pourraient être défectueux, comme l'internalisation du récepteur 5-HT_{1A}, situé sur les neurones sérotonergiques du noyau raphé dorsalis (NRD) (autorécepteurs) et les neurones non-sérotonergiques des domaines de projection du NRD comme l'hippocampe (hétérorécepteurs). Une fois activé, l'autorécepteur 5-HT_{1A} est internalisé, un processus démontré chez le rat par la microscopie électronique. Pour l'étude courante, nous avons utilisé la microTEP pour mesurer la liaison du [^{18}F]MPPF à l'autorécepteur dans le NRD du rat suivant son internalisation, incitée par la fluoxétine. Bien que l'internalisation ait été démontrée dans un sous-échantillon de rats en utilisant la microscopie électronique, la microTEP n'a pu détecter la baisse de liaison anticipée de l'autorécepteur dans le NRD suite à l'administration de fluoxetine. Nous proposons que la résolution de la microTEP, combinée à la taille du NRD du rat, ne permettent pas de détecter l'internalisation.

Key words (other than in title): binding potential – fluoxetine – immuno-electron microscopy - resolution

INTRODUCTION

The indoleamine neurotransmitter-modulator serotonin (5-hydroxytryptamine, 5-HT) plays an important role in the brain, subserving several physiological processes such as neuroendocrine responses, body temperature regulation, sleep, aggressive and sexual behaviour, mood, appetite and neurogenesis (e.g., Passchier and van Waarde, 2000a; 2000b; Lanfumey and Hamon, 2004). The following sections will review evidence linking 5-HT function to psychopathology as well as environmental and biological factors contributing to vulnerability to psychopathology. Next, we will review a putative neural mechanism that may, when faulty, underlie 5-HT transmission dysfunction, the internalization of a particular 5-HT receptor, the 5-HT_{1A} receptor. We will then examine methods that have been used to study internalization in the past, that is, immuno electron-microscopy and the insertion of β microprobes in rat, as well as PET in both cats and humans. We will conclude the introduction with the objective of the current study, namely to study internalization using microPET in rat.

Serotonin and psychopathology

Studies to date have established a strong link between impaired 5-HT function and various psychopathologies including mood (Blier and de Montigny, 1994; Cryan and Leonard, 2000), anxiety (Nutt and Stein, 2006), and eating disorders (Kaye, 2008; Kaye et al., 2005), as well as impulsive aggression in both humans (e.g., Pattij and Vanderschuren, 2008) and animals (e.g., Higley and Linnoila, 1997). Depressed patients have been reported to have low plasma levels of the 5-HT precursor L-tryptophan (Coppen et al., 1973; Cowen et al., 1989) and cerebrospinal fluid levels of the 5-HT metabolite, 5-HIAA (Millan, 2006), whereas tryptophan supplementation in depressed patients appears to be beneficial (van Praag et al., 1972; Meyers,

2000). In remitted patients, dietary tryptophan depletion induces a recurrence of symptoms, particularly when the depressive episodes are themselves recurrent (Delgado et al., 1990; Booij et al., 2002; Neumeister et al., 2004, 2006). Reduced 5-HT activity also increases aggression (Higley and Linnoila, 1997), while increased 5-HT function, by means of tryptophan supplementation, 5-HT reuptake inhibitors or 5-HT_{1A} and 5-HT_{1B} receptor activation, decreases aggression (Higley and Linnoila, 1997; Nelson and Trainor, 2007). The 5-HT system also appears to be implicated in anxiety and eating disorders. 5-HT_{1A} receptor (5-HT_{1A}R) knockout mice demonstrate a tendency to respond to novelty with fear and avoidance (Ramboz et al., 1998; Toth, 2003). A polymorphism in the gene encoding the 5-HT_{1A}R shows significant associations with agoraphobia, panic disorder and depression (Rothe et al., 2004). Moreover, the binding of the 5-HT_{1A} receptor antagonist [^{11}C]*N*-(2-(1-(4-(2-Methoxyphenyl)-piperazinyl)ethyl)-*N*-pyridinyl)cyclohexanecarboxamide ([^{11}C]WAY 100635) has been shown, with positron emission tomography (PET), to be lower in the raphe nuclei of untreated individuals with panic disorder compared to controls (Nutt and Stein, 2006). Likewise, patients with anorexia nervosa were found to have reduced cerebrospinal fluid concentrations of 5-HT metabolites, whereas remitted anorexics were found to have increased concentrations (Kaye et al., 2005). Furthermore, increased 5-HT_{1A} activity has been found in patients suffering from bulimia nervosa (Tiihonen et al., 2004) and anorexia nervosa (Bailer et al., 2005) using PET in combination with [^{11}C]WAY 100635. Medications acting on the 5-HT system, particularly the selective serotonin reuptake inhibitors (SSRIs), are often effective in treating patients with mood (Fuller, 1995; Nemeroff and Owens, 2002; Lanfumey and Hamon, 2004), anxiety (Lanfumey and Hamon, 2004; Irons, 2005; Davidson, 2006), eating (Irons, 2005), or impulse control

disorders (Coccaro, 1996; Moeller et al, 2001; Grant and Potenza, 2004), thus providing further evidence that 5-HT function is linked to various psychopathologies.

Diverse environmental insults may contribute to 5-HT neurotransmission dysfunction. Proper 5-HT function appears to be especially important early in life in the mammalian brain (Whitaker-Azmitia, 2001; Gaspar et al., 2003). Abnormal 5-HT tone early in life, whether increased or decreased, as a result of insult such as stress, social enrichment or isolation, maternal drug use, viral infections, and malnutrition (Whitaker-Azmitia, 2001), may modulate brain pathway development, differentiation and maturation. Moreover, stressful events early in life lead to depressive and anxiety disorders in later life as well as persistent abnormalities in hypothalamic-pituitary-adrenocortical (HPA) system functioning (reviewed in Ansorge et al., 2007). Disruption of maternal care in rodents has been shown to lead to both increased HPA activity and increased anxiety and depressive behaviors, whereas increased maternal care leads to opposite results (reviewed in Ansorge et al., 2007). Furthermore, increased or decreased 5-HT levels during different phases of development can cause long-lasting changes in neuronal differentiation and morphology (Whitaker-Azmitia, 2001). Adverse effects resulting from developmental 5-HT imbalances are observable in the adult and manifest as increased sensitivity to aversive stressors, negative life events, and vulnerability to developing disorders such as autism and anxiety disorders (Whitaker-Azmitia, 2001).

Genotype can also influence 5-HT function in later life. For example, polymorphisms exist which influence the amount of 5-HT transporter (5-HTT) expressed. Carriers of two long alleles (*l/l* genotype) express twice as many transporters as carriers of two short alleles (*s/s* genotype) (Wrase et al., 2006). Not only do human carriers of the *s* allele of the 5-HT transporter show reduced expression of the transporter, but they are also are more sensitive to

stress-induced activation of the amygdala, and are more prone to anxiety-like temperaments (Lesch et al., 1996) and to depressive recurrence as well as suicidal ideation or attempt in the context of environmental adversity (Caspi et al., 2003). Furthermore, a human polymorphism in the promoter region of the *htr1a* gene results in increased expression of presynaptic *htr1a* and decreased expression of postsynaptic *htr1a*, and is associated with increased anxiety and depression (Lemonde et al., 2003; Strobel et al., 2003). Interestingly, restoration of 5-HT_{1A}R in mice in early life, but not in adulthood, leads to normal anxiety levels (Gross et al., 2002), suggesting that 5-HT_{1A}R play a significant role in the maturation of the 5-HT system.

GPCR trafficking

Irrespective of cause or timing, multiple mechanisms involved in 5-HT neurotransmission may, when faulty, eventually lead to metabolic and psychiatric disease. One such mechanism is, speculatively, receptor internalization, a feature of G protein coupled receptor (GPCR) trafficking. G protein coupled receptors (GPCRs) constitute a large family of ~900 members mediating most cellular responses to hormones and neurotransmitters as well as vision, olfaction and taste (Wolfe and Trejo, 2007). Commonly known members include the α- and β-adrenergic receptors, all dopamine receptors, the muscarinic acetylcholine (ACh) receptors, the γ-aminobutyric acid B ($GABA_B$) receptors, certain glutamate and serotonin receptors, receptors for neuropeptides, as well as the odorant receptors and rhodopsin. Of interest, they are the targets of almost half of the drugs currently in use or being developed for treatment of a wide range of human disease, including psychopathology (Marchese et al., 2008).

GPCRs are all characterized by seven transmembrane-spanning α-helical segments separated by alternating intracellular and extracellular loop regions. GPCRs also contain three

N-linked glycosylation motives in the N terminal domain, a conserved DRY sequence at the initial segment of the third cytoplasmic loop, and phosphorylation sites in the third and fifth cytoplasmic loops. Interestingly, its amino acid sequence is highly conserved across mammalian species, with 89% homology between human and rat (reviewed in Wolfe and Trejo, 2007; Rosenbaum et al., 2009).

GPCRs are composed of 3 subunits: the α, β and γ subunits, which are found at the cell surface. The β and γ subunits remain attached together at the cell surface and form the βγ complex. The α subunit is only loosely bound to the plasma membrane, is thus free moving and generally responsible for activating or inhibiting effector enzymes upon ligand binding to the receptor (Wolfe and Trejo, 2007). In the inactive state, a molecule of guanine diphosphate (GDP) is normally bound to the G protein complex. Upon activation, receptors undergo conformational changes, which result in the exposure of the cytoplasmic sequence and interaction with heterotrimeric G proteins. Activated GPCRs promote the exchange of GDP for guanine triphosphate (GTP) on the α-subunit. This leads to the dissociation of the Gα subunit from the Gβγ subunits. The Gα subunit can then signal to a variety of effector enzymes, leading to downstream signaling, desensitization and/or internalization, the main processes of GPCR trafficking (reviewed in Wolfe and Trejo, 2007).

The quest to unraveling GPCR dynamics began with the endogenous β_2-adrenergic receptor (β_2AR). Internalization was shown to occur via the clathrin-dependent endocytic pathway (Moore et al., 2007). In short, activation of β_2AR causes phosphorylation of the receptor, translocation of arrestins to the plasma membrane and receptor uncoupling from G proteins within seconds (Wolfe and Trejo, 2007). More explicitly, G protein-coupled receptor kinases (GRKs), a family of protein kinases that specifically phosphorylate serine/threonine

residues within the C-tail of the third intracellular loop, phosphorylate activated receptors. Receptor phosphorylation leads to high-affinity binding and activation of β-arrestins, which then uncouple the receptor from the G protein and target the receptor to clathrin coated pits. Along with dozens of regulatory proteins, clathrin and adaptor proteins such as adaptor protein 2 (AP-2) are recruited at the cell surface and support coated pit assembly around the GPCR and invagination of the receptor. The GPCR is then enzymatically cleaved from the plasma membrane into the cytoplasm by the GTPase dynamin and the receptor is internalized. Activated receptors are separated from G proteins and signaling effectors at the cell surface, and the receptors are then targeted to early endosomes (reviewed in Wolfe and Trejo, 2007; Marchese et al., 2008).

Once internalized, the receptor is either degraded or recycled back to the plasma membrane. Degradation occurs when the receptor is directed towards late endosomes and ultimately lysosomes. Alternatively, the agonist dissociates from the receptor, G proteins are dephosphorylated and recycled back to the cell surface in a resensitized, functional state (reviewed in Moore et al., 2007; Wolfe and Trejo, 2007; Marchese et al., 2008). Whether any specific receptor will be sorted towards degradation or recycling is not known, but the prevailing theory suggests that differential receptor-arrestin affinity and trafficking mediate postendocytotic receptor sorting to recycling or degradative pathways (Moore et al., 2007).

Consequences ensue when GPCR internalization is faulty. Dysregulated GPCR trafficking is associated with disease in human. For example, patients with nephrogenetic diabetes insipidus show reduced or complete loss of renal epithelial GPCR vasopressin receptor (V_2R) surface expression, attributed to multiple V_2R mutations that impair trafficking through the biosynthetic pathway. Moreover, many GPCRs are over-expressed in human cancers and

contribute to tumor progression. Dysregulated trafficking of chemokine (C-X-C motif) receptor 4 (CXCR4) and protease activated receptor 1 (PAR1) within the endosomal-lysosomal system contributes to increased surface expression in breast cancer cells and cancer progression (Marchese et al., 2008). Recently, it has also been shown that mononuclear leukocytes of patients with major depression exhibit decreased immunoreactive amounts of β-arrestin-1. Interestingly, the decrease in β-arrestin-1 is correlated with symptom severity. Furthermore, it was demonstrated in rats that antidepressant medications including fluvoxamine increase β-arrestin-1 levels in both cortex and hippocampus (Avissar et al., 2004). It thus appears that different steps involved in GPCR trafficking may be faulty and eventually be associated with disease states. Problems may be as diverse as the variety of steps that could go awry.

The 5-HT_{1A} receptor

Since the description of GPCR trafficking in β_2AR, this process has been demonstrated in a variety of receptors, including the 5-HT_{1A}R (Raymond et al., 1999). Here, we are specifically interested in the internalization of the 5-HT_{1A}R receptor. Given the evidence that GPCR trafficking may be dysfunctional in different ways and in turn linked to disease states, it is conceivable that faulty 5-HT_{1A}R internalization may lead to abnormal 5-HT neurotransmission, and ultimately, abnormal mood and behavior.

The 5-HT_{1A}R is a subtype of serotonin receptors. Fourteen serotonin receptor subtypes mediating the effects of 5-HT in mammalian brain have thus far been identified by pharmacological and biomolecular techniques (Barnes and Sharp, 1999). These 5-HT receptors are subdivided into 6 distinct G protein-coupled receptor classes: $5HT_1$, 5-HT_2, 5-HT_4, 5-HT_5, 5-HT_6 and 5-HT_7 as well as one class of ligand-gated ion channel receptors, the 5-HT_3 family. The

5-HT_1 family itself comprises five receptor subtypes: 5-HT_{1A}, 5-HT_{1B}, 5-HT_{1D}, 5-HT_{1E} and 5-HT_{1F}. It is the largest family of 5-HT receptors, originally grouped together because of their high affinity for 5-HT. The 5-HT_{1A} receptor (5-HT_{1A}R) subtype is a 422 amino acid protein encoded in a single intronless gene (chromosome 5, q11-2-q13) with typical GPCR features including seven transmembrane domains (Fargin et al., 1998; Albert et al., 1990; reviewed in Nichols and Nichols, 2008).

Though there is no brain region without 5-HT innervation (Steinbusch, 1981), 5-HT_{1A}R are particularly abundant in the dorsal raphe nucleus (DRN), the principal site of origin of 5-HT cell bodies, and in territories of 5-HT projection, such as hippocampus, lateral septum, entorhinal and frontal cortex. They are less abundant but still present in thalamic and hypothalamic nuclei, and hardly detectable in the substantia nigra and cerebellum (Kia et al., 1996; Lanfumey and Hamon, 2004; reviewed in Barnes and Sharp, 1999). 5-HT_{1A}R mRNA is found in the same regions as the receptor itself, with the highest density in the limbic system, suggesting that 5-HT_{1A}R are not transported away from their region of synthesis (Lanfumey and Hamon, 2004), and therefore located onto neuronal soma-dendrites.

In 5-HT nuclei of origin, such as the DRN, 5-HT_{1A}R are located on the 5-HT neurons themselves (autoreceptors), whereas in territories of projection, such as hippocampus, they are located on non 5-HT neurons innervated by 5-HT, and can therefore be considered as heteroreceptors. Irrespective of the type of 5-HT_{1A} receptor, its activation induces a membrane hyperpolarization and diminishes neuronal excitability via direct interactions with G proteins and ion channels (Sprouse and Aghajanian, 1987). Thus, in the DRN, the 5-HT_{1A} autoreceptors (5-HT_{1A}autoR) negatively control the firing and hence the release of 5-HT (Sprouse and Aghajanian, 1987), whereas in the territories of 5-HT innervation, they mediate the 5-HT

inhibition of non 5-HT neurons. Immuno-electron microscopic studies have revealed that in both locations, 5-HT_{1A}R are mostly located on extrasynaptic portions of the plasma membrane of 5-HT or non 5-HT cell bodies and dendrites (Riad et al., 2000).

Activation of 5-HT_{1A}autoR allows for the study of internalization. Activation of the 5-HT_{1A}autoR can be done either using an agonist such as 8-hydroxy-*N*,*N*-dipropyl-2-aminotetralin (8-OH-DPAT), or indirectly, by increasing serotonin levels, such as is the case following SSRI administration. Specifically, acute administration of an SSRI such as fluoxetine increases the extracellular concentration of 5-HT in the DRN and its territories of projection (Rutter and Auerbach, 1993; Fuller, 1994; Kreiss and Lucki, 1995; Malagié et al., 1995; Rutter et al., 1995; Hervás and Artigas, 1998). The resulting activation of 5-HT_{1A}autoR leads to increased conductance of potassium ions and decreased high-threshold calcium current. This response is G protein-mediated, and ultimately inhibits the firing of 5-HT neurons (Blier and de Montigny, 1987; Sprouse and Aghajanian, 1987; Cunningham and Lakoski, 1990; Rigdon and Wang, 1991; Lanfumey et al, 1993; Dong et al, 1997; Czachura and Rasmussen, 2000) and consequently the release of 5-HT in both the DRN (Adell et al, 2002) and its territories of projection (Kennett et al., 1987; Hamon et al., 1988; Hutson et al., 1989; Sharp et al., 1989; Bohmaker et al., 1993; Invernizzi et al., 1996; Sharp et al., 1996; Adell et al., 2002) (reviewed in Barnes and Sharp, 1999; Piñeyro and Blier, 1999). A rapid and transient desensitization of 5-HT_{1A}autoR (but not heteroreceptors) follows, evidenced by a diminished responsiveness of DRN neurons to the 5-HT_{1A} receptor agonist 8-OH-DPAT (Kennett et al., 1987; Beer et al., 1990; Le Poul et al., 1997; Seth et al., 1997). These effects are blocked by the selective 5-HT_{1A}R antagonist, WAY 100635 (Corradetti et al., 1996), which by itself has no effect on the firing of 5-HT neurons (Mundey et al., 1994; Corradetti et al., 1996; Martin et al., 1999).

The in vitro study of 5-HT$_{1A}$ autoreceptor trafficking

Immuno-electron microscopic studies carried out in rats examined one hour after the acute administration of the 5-HT$_{1A}$R agonist, 8-OH-DPAT or the SSRI fluoxetine, have shed new light on these results (Riad et al., 2001; 2004). These authors had demonstrated that 1 hour following the administration of a single dose of 8-OH-DPAT or fluoxetine, there was a partial and reversible internalization of 5-HT$_{1A}$autoR in DRN neurons, evidenced by a 30-40% reduction in the density of 5-HT$_{1A}$R immunoreactivity on the plasma membrane of their cell bodies and dendrites and a corresponding increase in their cytoplasm (Riad et al., 2001; 2004). This decrease occurred only in the DRN and was absent in areas of projection such as hippocampus. Furthermore, this decrease could be observed as soon as 15 minutes after the injection of either drug, was not cumulative when both drugs were injected at the same time, was of the same magnitude 1 hour after their administration, was blocked by prior administration of the 5-HT$_{1A}$R antagonist WAY 100635, and was no longer apparent after 24 hours. Twenty four hours after either 8-OH-DPAT or fluoxetine administration, the receptors had returned to normal levels on the plasma membrane, and could again internalize upon the administration of 8-OH-DPAT (Riad et al., 2008). It was thus clear that the short-term, partial and transient desensitization of 5-HT$_{1A}$autoR, demonstrated by prior electrophysiological and pharmacological studies carried out under the same conditions, was associated with an internalization of these receptors.

The in vivo study of 5-HT$_{1A}$ autoreceptor trafficking

In the course of these studies, it was deemed of interest to concomitantly examine the binding of 4-(2'-methoxyphenyl)-1-[2'-[N-2"-pyridinyl)-*p*-[(^{18})F]fluorobenzamido]ethyl]

piperazine ([^{18}F]MPPF) (Zhuang et al., 1994), an antagonist and specific radioligand of 5-HT_{1A}R which allows for the *in vivo* imaging of the 5-HT_{1A} receptors in both animals and humans (Passchier et al., 2000a; 2000b; Plénevaux et al., 2000; Passchier and van Waarde, 2001; Shively et al., 2006; reviewed in Aznavour and Zimmer, 2007). Both the *in vitro* and the *in vivo* biodistribution of [^{18}F]MPPF labeling are in agreement with the known distribution of 5-HT_{1A} receptors. Of relevance, very high [^{18}F]MPPF binding has been found in the DRN and hippocampus, and very low binding in the cerebellum (Passchier and van Waarde, 2001; Passchier et al., 2000a; 2000b). Furthermore, *in vitro* and *in vivo* studies performed in animals demonstrated that [^{18}F]MPPF labeling in the brain is reversible and characterized by very low non-specific binding (Passchier et al., 2000a; 2000b). Another interesting property of [^{18}F]MPPF is that its affinity for 5-HT_{1A} receptors is 3.3 nmol/L (Zhuang et al., 1994), which is quite similar to that of 5-HT for 5-HT_{1A} receptors (4.17 nmol/L; Van Wijngaarden et al., 1990). Finally, [^{18}F]MPPF has been used in both animals (Le Bars et al., 1998), and more recently in humans, as a radioligand for PET measurements of 5-HT_{1A} binding potential (an index of unbound 5-HT_{1A} receptors) (Passchier et al., 2000a; 2000b).

The measurement of [^{18}F]MPPF binding could be done in rat during immunocytochemical studies such as described above, using ß microprobes implanted in the immediate vicinity of the DRN and into the hippocampus. Using this approach, a selective lowering in the *in vivo* binding of [^{18}F]MPPF was measured in the DRN, and was associated with the internalization of the 5-HT_{1A}autoR after acute treatment with either 8-OH-DPAT (Zimmer et al, 2004) or fluoxetine (Riad et al., 2004). This lowering was of the same magnitude as the decrease in plasma membrane density of the immunolabeling of 5-HT_{1A}autoR in DRN (30-35%), was blocked by pretreatment with WAY 100635, and occurred despite the fact that the total

amount of radioactivity measured in the DRN by *in vitro* radioautography (on film) appeared to be the same as in untreated rats. Again, there was no change in hippocampus.

On the basis of these results, a series of [^{18}F]MPPF PET experiments were undertaken. A first PET study carried out by Aznavour et al. (2006) demonstrated the possibility of detecting and measuring the selective decrease in [^{18}F]MPPF binding taking place in the DRN of cats, following the intra-peritoneal administration of a single dose of fluoxetine (20 mg/kg). This decrease in binding was accompanied by decreases in the regional activity-time curves to values approaching those of the cerebellum, and was not seen in hippocampus acutely or in either regions following chronic treatment. A subsequent study by Sibon et al. (2008) demonstrated a similar decrease in the specific binding of [^{18}F]MPPF in the DRN of healthy adult men administered a single 20 mg oral dose of fluoxetine (Prozac®). In eight subjects, the administration of fluoxetine elicited a 44% ± 22 decrease in [^{18}F]MPPF binding potential (BP_{ND}, according to Innis et al., 2007) five hours after the randomized double-blind administration of the drug versus placebo. In view of the preclinical results and of the lack of change in [^{18}F]MPPF BP in any other brain regions, such a decrease was most likely attributable to 5-HT_{1A}autoR internalization.

Very recently, studies demonstrated the possibility of using [^{18}F]MPPF and small animal PET (microPET) to measure 5-HT_{1A}R binding potential in different regions of the rat brain, including the midbrain raphe nuclei (Aznavour et al. 2009; Moulin-Sallanon et al., 2009). In Aznavour et al. (2009), values of BP_{ND} at baseline were measured for hippocampus, entorhinal cortex, septum, medial prefrontal cortex, amygdala, raphe nuclei, paraventricular hypothalamic nucleus and raphe obscurus, which were in the same range as those previously reported in cat, non human primates and human (Passchier et al., 2000a; 2000b; Plénevaux et al., 2000;

Passchier and van Waarde, 2001; Costes et al., 2005; Aznavour et al., 2006). Test-retest variability was in the order of 10% in the larger brain regions (hippocampus, medial prefrontal and entorhinal cortex), and less than 20% in small nuclei such as the septum and the paraventricular hypothalamic, basolateral amygdaloid and raphe nuclei.

MAIN OBJECTIVE

In this context and because microPET brain imaging of 5-HT_{1A}R with [^{18}F]MPPF might open a novel methodological avenue for investigating 5-HT_{1A}R function in the rat, it was deemed worthwhile to determine if it could be used to detect and measure the selective decreases in binding associated with the fluoxetine-induced internalization of 5-HT_{1A}autoR in the rat DRN. It was hypothesized that a lowering in [^{18}F]MPPF binding potential (BP_{ND}) would be found in the DRN (but not hippocampus or other 5-HT projection areas), in response to acute fluoxetine treatment.

MATERIALS AND METHODS

Acute fluoxetine treatment

Ten adult male Sprague Dawley rats, weighing 200-250 g at the study onset, were obtained from Charles River Laboratories (St-Constant, QC). Rats were housed individually at a constant temperature of 20-22°C under a 12 h light/dark cycle with free access to food and water. All animal procedures were conducted in accordance with the guidelines of the Canadian Council on Animal Care. Each animal underwent two PET measurements with [^{18}F]MPPF: untreated, and following administration of an acute dose of fluoxetine (10 mg/kg, i.p.) one hour prior to the [^{18}F]MPPF injection. Scans were performed one (5 rats) or two (5 rats) weeks apart

(see Fig. 1 for time line). The order was the same in all rats: the first scan was untreated and the second followed acute fluoxetine, in order to avoid carry over effects of the drug. Fluoxetine was obtained from Sigma-Aldrich (Oakville, ON).

PET procedure

The microPET measurements were performed at the Montreal Neurological Institute, assisted by an animal health technologist from the MNI Animal Care Facility. Each rat underwent two scans of 60 minutes each, with an interval of one or two weeks between scans. Rats were collected from the animal care facility 1-2 hours prior to scanning in order to give them time to acclimatize to the new environment and avoid effects of stress as much as possible. All scans were performed under general anesthesia, induced by a mixture of ketamine (100 mg/kg, i.p.) and midazolam (2 mg/kg, i.p.), followed by isoflurane (1-2%), delivered in an O_2/air mixture, which was administered through a nose cone connected to a rodent vaporizer (CWE, inc. model EFM-1). A small amount of ophthalmic ointment was applied to each eye to prevent ophthalmic lesions. Once under general anesthesia, the animals were placed on a pre-warmed operating stereotaxic head holder, with their head in the centre of the microPET's field of view. They were constantly monitored for signs of pain, heart rate and rectal temperature throughout the scan (Biovet physiological monitoring), and ventilation parameters were adjusted as needed, by the animal technologist. Once scanning was completed, rats were allowed to recover under observation for 30-60 minutes and then returned to their home cages in the animal care facility.

[^{18}F]MPPF was synthesized at the Montreal Neurological Institute cyclotron unit according to standard techniques (Le Bars et al., 1998) and injected in the tail vein. PET measurements were obtained on the microPET R4 scanner (CTI, Concorde Microsystems, LLC).

A 10-minute transmission scan was followed by a bolus injection with 37 Mbq (1 mCi) in 0.1 ml of [^{18}F]MPPF and a dynamic acquisition of 60 minutes divided into 27 frames (6 frames with 10 seconds, 3 frames with 20 seconds, 8 frames with 60 seconds, 4 frames with 300 seconds, 3 frames with 600 seconds and 2 frames with 900 seconds). Images were reconstructed using Fournier rebinning followed by 2-dimensional filtered back projection with a ramp filter cutoff at Nyquist frequency.

PET analysis

In keeping with Aznavour et al. (2009), dynamic PET volumes from 0 to 60 minutes were integrated and manually co-registered with MRI data acquired from a single male Sprague Dawley rat weighing 250 g (Élevage Dépré, Saint Doulchard, France) (Register 1.3.6 and Minc-2.0.9, MNI-BIC software, Montreal, QC) using a rigid body transformation with 6 degrees of freedom. The obtained transformation matrix was then applied to the dynamic PET volumes. A 20 mm^3 ellipse was drawn in the centre of the caudal area of the cerebellum on the co-registered MRI (Display 1.3, MNI-BIC software), in order to estimate the binding parameters of the tracer according to the simplified reference tissue model (SRTM) (Millet et al, 2008). The SRTM model is based on the analytic solution of the compartment model for estimating three parameters without the use of an arterial sampling input function. BP is the ratio of available receptor density to receptor affinity. The cerebellum white matter was used as a reference region, since it contains few 5-HT$_{1A}$ receptors in the adult rat (Pazos and Palacios, 1985). Parametric images of binding potential were calculated from individual voxel time-activity curves using Receptor Parametric Mapping Software. BP volumes were automatically co-registered using PET-to-PET cross-correlation with 7 degrees of freedom (mni_autoreg-0.99.3,

MNI-BIC Software). All 10 PET volumes of BP were then averaged into a single volume, which was fused with the MRI to draw the regions containing binding and regrouped into anatomical VOIs (Display-1.3, MNI-BIC Software). The Paxinos and Watson stereotaxic atlas of the rat brain was used to identify regions of interest on the MRI and draw the corresponding VOIs. The regions were the medial prefrontal cortex (27 mm^3), septum (8 mm^3), hippocampus (100 mm^3), raphe nuclei (3 mm^3), entorhinal cortex (15 mm^3), amygdala (7 mm^3), paraventricular hypothalamic nucleus (4 mm^3), and raphe obscurus (2 mm^3). Regional radioactivity concentration (kilobecquerel per cubic centimeter) was also measured in the dynamic PET volumes for each VOI and plotted versus time.

Co-registered parametric images of BP were smoothed with a 1 mm Gaussian blur, and a voxelwise paired *t* test was performed in SPM5 (Wellcome Trust Centre for Neuroimaging at UCL, UK) to examine differences across conditions. Student's two-tailed *t* test was also used to assess regional differences in BP across pharmacological conditions.

Immunocytochemical procedure

Two of the rats subjected to [^{18}F]MPPF/PET in the fluoxetine condition and another which was not included in the imaging analyses (since it died during the scan), as well as three age-matched controls, were examined by immuno-electron microscopy, to determine and quantify the subcellular localization of 5-HT_{1A} receptors in the DRN. The required chemical fixation of the brain was performed immediately after completion of the image acquisition phase in the fluoxetine-treated rats subjected to PET, with the animals deeply anesthetized with sodium pentobarbital (80 mg/kg, i.p). Fixation of the brain was by aortic arch perfusion with 3.5% acrolein and 4% paraformaldehyde (PFA) in 0.1 M phosphate buffer (PB, pH 7.4). The brain

was removed and postfixed for 60 minutes in 4% paraformaldehyde in PB. Transverse sections (40 μm thick) containing the NRD and the ventral blade of hippocampus were cut using a vibrating microtome, treated with 0.5% sodium borohydride in 50 mM phosphate buffered saline (pH 7.4), then processed for pre-embedding immunogold labeling of 5-HT_{1A} receptors and electron microscopy. Sections from both fluoxetine treated and control rats were processed together in keeping with Riad et al. (2004).

Free-floating sections were pre-incubated for 60 minutes in blocking solution, incubated overnight at room temperature in rabbit 5-HT_{1A} receptor antiserum (1:1000 dilution) (Riad et al., 1991) followed by 2 hours in goat anti-rabbit IgG conjugated with 1 nm gold particles (1:50, AuroProbeOne, Amersham Biosciences, Oakville, ON). After several washes in PBS and sodium acetate, the immunogold signal was intensified with silver (IntenSE-M kit, Amersham Biosciences), the sections were postfixed in 1% osmium tetroxide, dehydrated in ethanol and flat-embedded in Durcupan (Sigma-Aldrich, Oakville, ON, Canada) between two sheets of Aclar plastic (EMS/Cedarlane, Homby, ON, Canada). After polymerization, a rectangular portion of sections containing the DRN were excised from the Aclar sheets and fixed to the tip of resin blocks. Ultrathin silver-gold sections were then cut, collected on naked copper grids, counterstained with Reynold's lead citrate and uranyl acetate and examined with the electron microscope (Philips CM100, 60 kV). Approximately one week is needed to complete processing of one rat.

Immunocytochemical analysis

As in Riad et al. (2000, 2004, 2008), the analysis focused on dendritic profiles displaying 5-HT_{1A} immunoreactivity. Only dendritic profiles bearing three or more silver-intensified

immunogold particles were considered as labeled. Electron microscopic images of thirty or more labeled dendrites per rat were photographed at a working magnification of 6,800 X, and printed at a final magnification of 17,000 X.

On the prints, two cellular compartments were defined: a membrane compartment corresponding to a narrow zone under the membrane, 30 nm in thickness, corresponding to the average size of immunogold particles, and a cytoplasmic compartment encompassing the rest of the perikaryal or dendritic cytoplasm. The number of labeled particles in each compartment was determined manually. The diameter and circumference of the dendritic profiles were then measured with the aid of a computerized image analysis system (NIH Image 1.60), and the results first expressed as labeling density, i.e. the number of particles per surface unit for both the membrane and the cytoplasmic compartments. In a second step, the distribution of receptors in the plasma membrane versus cytoplasmic compartment of NRD dendrites was expressed as percentage of control, to avoid differences that might merely reflect technical variations from one experimental session to another. Treatment effects were assessed using a Student's *t* test. Differences were considered significant if $p < 0.05$.

RESULTS

As recently reported in normal rat (Aznavour et al., 2009), parametric receptor mapping of [^{18}F]MPPF binding with the microPET allowed the visualization and measurement of 5-HT_{1A}R BP_{ND} in various brain regions of untreated and fluoxetine-treated rat, including the midbrain raphe and raphe obscurus nuclei (Fig. 2, Fig. 3 and Table 1). BP_{ND} represents the ratio of specifically bound radioligand to that of non-displaceable radioligand in tissue at equilibrium (reviewed in Innis et al., 2007). More generally, BP_{ND} allows for the comparison of radioligand

concentrations in receptor-rich to receptor-free regions and is thus commonly used in reference tissue methods. As shown in Table 1, the average baseline BP_{ND} values measured in the present study were similar to those previously reported (Aznavour et al., 2009) for each of these same regions, and not significantly different in any region between untreated and fluoxetine-treated rats. Percent change between fluoxetine and untreated conditions was 5.61% in raphe nuclei, 4.12% in the raphe obscurus, 8.61% in the hippocampus, 8.55% in the entorhinal cortex, 1.24% in the medial prefrontal cortex, 6.30% in the amygdala, 15.25% in the hypothalamus, 3.15% in the septum and 52.98% in the cerebellum. Percent change was determined by subtracting the BP_{ND} value following fluoxetine administration from the BP_{ND} value in the untreated condition, then dividing the whole by the BP_{ND} value following fluoxetine and multiplying by 100. A positive value signifies a decrease in BP following fluoxetine treatment, compared to the untreated condition, and a negative value indicates an increase following fluoxetine treatment. Based on immuno-electron microscopy results (e.g. Riad et al., 2001; 2004), we would expect a change of 35% in the DRN and no change in projection areas. The small differences found across experimental conditions were more consistent with test-retest values as found in Aznavour et al. (2009) then with differences induced by pharmacological manipulation. Indeed, percentage change in Aznavour et al. (2009) were 10.2% in the raphe nuclei, 2.6% in the raphe obscurus, 2.4% in the hippocampus, 2.6% in the entorhinal cortex, 8.5% in the medial prefrontal cortex, 0.3% in the amygdala, 1.7% in the hypothalamus, and 5.5% in the septum. Given that BP_{ND} values were low under both conditions in the current study (e.g. 0.5 ± 0.09 untreated and 0.5 ± 0.07 in raphe nuclei following fluoxetine administration), it is possible that BP_{ND} values were under- or over-estimated. Furthermore, as shown in Fig. 4, there was no consistency in the direction and amplitude of changes in DRN BP_{ND} values between untreated and fluoxetine

treatment conditions in individual rats. Whereas, in hippocampus, only 2 of the 10 individual values appeared to be higher after fluoxetine administration and the others showed minimal change, the variations in DRN were in both directions and much greater in 4 of the 10 rats. The results are in contrast with our expected results of a small decrease in BP_{ND} in raphe nuclei following fluoxetine administration, compared to the untreated condition.

In the three rats whose brain was fixed within minutes after the end of the fluoxetine scan and processed for 5-HT_{1A}R immuno-electron microscopy (including a rat that died after 40 min of scanning and was not included in the BP measurements), internalization of the 5-HT_{1A}autoR was observed in the DRN (Fig. 5). As in earlier studies following acute fluoxetine administration (Riad et al., 2004), a much lower number of silver-intensified immunogold particles was then observed along the plasma membrane of DRN dendrites and a greater number in the cytoplasm by comparison to control. When the control values of plasmalemmal labeling were set at 100% to normalize the data, the internalization was equivalent to a 34 ± 1.5 % (mean ± SEM) decrease in density of the immunogold labeling of the plasma membrane of dendrites, with a corresponding increase (threefold) in density of cytoplasmic labeling (Table 2). In detail, the average number of silver-intensified immunogold particles per surface unit of fluoxetine-treated rats were multiplied by 100 and divided by the average number of particles of untreated rats for each experiment pair. By then subtracting these values from 100, we obtained the corresponding % decrease in average number of particles for each experiment. The mean and standard error of the mean for the three rats was calculated and used to conduct a t-test. The mean percent change was significant with t=3.535 and p=0.024.

DISCUSSION

A recent study (Aznavour et al., 2009) has already demonstrated that microPET imaging (R4, Concorde Microsystems) of the radioligand [^{18}F]MPPF permits the measurement of BP_{ND} to 5-HT_{1A} receptors in different regions of rat brain, including the midbrain raphe nuclei, where these somatodendritic receptors are known to act as autoreceptors. As in this prior study, a validated simplified reference tissue model (SRTM) (Gunn et al., 1998) was used to generate parametric images of binding potential values (BP_{ND}), according to the consensus nomenclature (Innis et al., 2007). Cerebellar white matter, which is assumed to be devoid of 5-HT_{1A}R specific binding (Parsey et al., 2005) was used as reference region.

The present study sought to determine whether the microPET could detect and measure the selective 30-40% decrease in [^{18}F]MPPF BP_{ND} expected from the internalization of 5-HT_{1A}autoR in the midbrain raphe nuclei of rat after acute treatment with the prototypic SSRI fluoxetine. The major conclusion from the present experiments is that the current resolution of the microPET machine cannot reliably detect a change of this amplitude in an anatomical area as small as the rat DRN.

It is conceivable that internalization did not occur in this particular experiment, but the results of the immunocytochemical method strongly argue against this possibility. Immuno electron microscopy is a validated, often-used method allowing for the visualization of internalization from the cell membrane into the cytoplasm (e.g. Riad et al., 2001; 2004). The most likely explanation is thus that internalization occurred following acute administration of fluoxetine in comparison to the untreated condition in the present experiment, but that it could not be detected using microPET.

This study made use of the R4 Concorde microPET scanner (Concorde Microsystems Inc.), an instrument dedicated to small animal imaging and, specifically, imaging in rodents. As detailed in Knoess et al. (2003), this small animal scanner yields an axial field of view (FOV) of 78 mm and a ring diameter of 148 mm, with the electronic FOV restricted to a diameter of 100 mm in the transaxial direction. The volumetric resolution is better than 15.6 µl within 20 mm of the center of the FOV. With a crystal size of 2.1 x 2.1 x 10 mm^3 and a center-to-center distance of 2.4 mm, the spatial resolution is approximately 2 mm at the center of the tomograph. In fact, the spatial resolution in the center was measured at 1.84 mm full width half maximum (FWHM) in the axial direction, 1.65 mm FWHM in the radial direction (vertical direction of the FOV), and 1.66 mm FWHM in the tangential direction (horizontal direction of the FOV). Of course, resolution deteriorates with increased distance from the FOV. The scanner is also equipped with a 25-mm-thick external lead shield, which confines the animal port on both sides to an opening of 120 mm to decrease scatter contribution from out-of-FOV activity. Given greater resolution than larger PET scanners designed for humans, the R4 Concorde microPET scanner appears adequately suited to assess BP in most anatomical regions of rat brain.

As in all other mammals, the largest population of 5-HT cell bodies in rat brain is that of the DRN, which comprises approximately 11,500 5-HT cell bodies in the rat, i.e., one third of its total neuronal population (Descarries et al., 1982; reviewed in Pineyro and Blier, 1999). Other neurotransmitters found to co-localize in the raphe nuclei include dopamine, γ-aminobutyric acid (GABA) and peptidergic and nonpertidergic transmitters such as substance P (reviewed in Pineyro and Blier, 1999). As delineated by its 5-HT cell population, the rat DRN is roughly shaped as an elongated losangic volume, which extends for 3 mm rostrocaudally, but is very narrow (200 µm) in its rostral and caudal extremities and is only 1 mm wide, i.e. 0.5 mm on each

side of the midbrain, in the largest extent (reviewed in Descarries et al., 1982). In most species, the DRN consists of several regions with different morphology, cell density and projections. Anatomical proximity between different 5-HT clusters allows for a network of interconnections among 5-HT neurons and a great amount of cross-talk (Pineyro and Blier, 1999). The other 5-HT nucleus in midbrain is the median raphe nucleus (MRN), which constitutes the second largest cluster of 5-HT neurons in the mammalian CNS (Pineyro and Blier, 1999), is more ventrally located, even narrower, and contains a smaller number of dispersed 5-HT neurons. In the midbrain, these two raphe nuclei appear to be the only ones containing neurons endowed with 5-HT_{1A} receptors.

As discussed by Gunn et al. (1998), even in man, the size and shape of the DRN complicate accurate sampling from this nucleus, leading to noisy ROI time activity curves and thus decreased accuracy of BP estimates. Given the limited resolution of the R4 Concorde microPET scanner and the size of the midbrain DRN in rat, BP_{ND} values obtained from this region are expected to be underestimated, due, at least in part, to the partial volume effect. The partial volume effect occurs when radioactive counts from a source or focus "spill out" into a region that is volumetrically larger in the reconstructed image than its physical size. Each PET scanner has an intrinsic point spread function (PSF) which is a profile of how much spread in a reconstructed image occurs when imaging a point source in air. The width of this PSF, which is characterized by measuring full width half maximum (FWHM), is usually used as a measure of spatial resolution. As long as objects of interest are greater than two times the FWHM, the partial volume effect is not very significant. However, if the object is less than two times the FWHM, as in the case of the rat midbrain nuclei, a significant fraction of the counts "spill out" of the reconstructed object (Srinivas et al., 2009). In other words, when a region of interest (ROI)

is smaller than twice the FWHM and surrounded by tissue deprived of potential binding sites, the recovery coefficient may be expected to be low. Not only is there a spillover of counts from the ROI to surrounding voxels (Hoffman et al., 1979), but also a reduction of the BP values attributed to the ROI because the low counts in the surrounding tissue contaminate the ROI. Partial volume correction methods have been developed to correct this effect as much as possible (e.g. Srinivas et al., 2009), but these are hardly applicable to a ROI as small as the rat DRN.

These combined limitations could account for the fact that, even if a relatively consistent [^{18}F]MPPF BP_{ND} measurement could be obtained from the midbrain raphe of untreated rat using the microPET, as reported in Aznavour et al. (2009), the 35% change in BP_{ND} due to internalization of 5-HT_{1A}autoR expected following acute fluoxetine administration may have gone undetected in the present experiment. The current lack of resolution of microPET machines could also explain the negative results of Moulin-Sallanon et al. (2009), who, similar to us, measured [^{18}F]MPPF binding in rat DRN following the acute and chronic administration of the SSRI citalopram, instead of fluoxetine, and found no apparent change in BP. Although binding could be measured in regions of interest including the DRN, hippocampus, cingulate cortex and frontal cortex, no significant difference was found following acute fluoxetine administration. Their result was not due to non-specific activity of the ligand, since these authors also reported a complete absence of [^{18}F]MPPF binding in the brain of 5-HT_{1A}R knockout mice.

It may have been possible to detect a significant difference had we have increased the sample size. To verify this assumption, based on the binding potential values obtained in the raphe nuclei, a power calculation for a paired samples *t* test (1 tailed) was done, with the alpha level set at 0.05 and the power at 0.80. The effect size for group differences in BP was

0.0798546. The power analysis indicated that we would need 971 subjects to detect a difference between untreated and fluoxetine-treated conditions. This provides further evidence that we are underpowered. Given that a sample size approaching 1000 animals is unrealistic and unethical, equipment with greater resolution, not currently available, would be needed to visualize and measure the decrease in BP associated with internalization of the 5-HT_{1A}autoR using microPET.

Our method of data analysis, like the parameters of the available microPET scanner, may have also contributed to the unreliability of the [^{18}F]MPPF BP measurement from rat DRN. In a recent study, Sullivan et al. (2009) used the two-tissue compartment model of analysis rather than the more conventional SRTM analysis method in order to assess [^{11}C]WAY 100635 BP to 5-HT_{1A}autoR in bipolar depression. Their outcome measure was BP_F rather than BP_{ND}, referring to the concentration ratio of specifically bound to free radioligand in tissue at equilibrium, with the free radioligand in tissue assumed to equal the free concentration in plasma if the ligand passes the blood brain barrier only by diffusion. In contrast, BP_{ND} refers to the ratio of specifically bound radioligand to that of non-displaceable radioligand in tissue at equilibrium (reviewed in Innis et al., 2007). BP_{ND} is commonly used in reference tissue methods, since it compares the concentration of radioligand in receptor-rich to receptor-free regions. However, when Sullivan et al. (2009) utilized both methods to analyze their data, they observed that the two-compartment model method was able to find significant changes in [^{11}C]WAY 100635 BP that the SRTM method could not detect. However, as found by Gunn et al (1998), better reproducibility is achieved by SRTM. The 2-tissue compartment model was a significantly better descriptor of the data but the parameter estimates have a larger variance due to the increased model order, which is not ideal for the comparison of BP across pharmacological

conditions. An increase in variance would bring doubt to results showing significantly different BP across pharmacological conditions.

It would be of interest to use the neurotoxin 5,7-dihydroxytryptamine (5,7-DHT) to destroy the 5-HT neurons residing in the rat DRN (Choi et al., 2004), thus eliminating all 5-HT_{1A} receptors in this midbrain region, and then determine whether a lowering in [^{18}F]MPPF binding would be measurable using the current microPET. The presence of labeling would signify that labeling in the present experiment was not specific to the 5-HT_{1A}R and possibly due to noise. Conversely, a total lack of binding would confirm the specificity of binding to the 5-HT_{1A}R and favor the view that it is the insufficient magnitude of the change after acute fluoxetine treatment which accounted for the "negative" results of the present experiments.

Alternatively, we could use another 5-HT_{1A}R radioligand to detect and measure the binding in DRN, such as the 5-HT_{1A} antagonist [*Carbonyl*-^{11}C]*N*-(2-(1-(4-(2-Methoxyphenyl)-piperazinyl)ethyl)-*N*-pyridinyl)cyclohexanecarboxamide ([^{11}C]WAY 100635). However, this radioligand possesses a higher lipophilicity ([^{11}C]WAY 100635 logD (pH 7.4) = 3.02 versus [^{18}F]MPPF logD (pH 7.4) = 2.81) (Elsinga et al., 2005) and shows a much greater affinity (inhibition constant K_i = 0.8 nmol/L) than [^{18}F]MPPF (K_i = 3.3 nmol/L) for the 5-HT_{1A}R (Zhuang et al., 1994). [^{18}F]MPPF was chosen because its affinity is more similar to that of 5-HT for 5-HT_{1A}Rs (K_i = 4.17 nmol/L; Van Wijngaarden et al., 1990) than [^{11}C]WAY 100635. Furthermore, [^{18}F]MPPF has a longer half-life (109.8 minutes) than [^{11}C]WAY 100635 (20 minutes) (reviewed in Passchier and van Waarde, 2001). It is not known whether [^{11}C]WAY 100635 binding would be similarly affected as that of [^{18}F]MPPF by the internalization of these receptors.

CONCLUDING REMARKS

The current methods available to us to image small regions of the rodent brain are still limited, and may thus not be adequate for measuring small but significant differences in BP_{ND} following pharmacological challenges. It is nonetheless conceivable that machines with a better resolution will eventually be available to obtain such measurements. If such technology was ever available, it would open new avenues of research for the investigation of the 5-HT_{1A}autoR functioning in both healthy and pathological states.

Serotonin related neuropsychiatric disorders including depression are disabling conditions (Brundtland, 2001) and SSRI medications used to treat depression are not always clinically effective (Fava, 2000). In the case of depression, even when effective, alleviation of depressed mood by SSRI takes 2-4 weeks (Blier and de Montigny, 1994). This effect is thought to be due to the desensitization of the 5-HT_{1A}autoR. Fifteen minutes following acute administration of fluoxetine, 35% of DRN 5-HT_{1A}autoR are internalized from the cell membrane to the cytoplasm (Riad et al., 2004) but following chronic treatment (3 weeks), there is no difference between treated rats and controls (Riad et al., 2008). This suggests that following repeated challenge and internalization, the 5-HT_{1A}autoR loses functionality. This could be due to an inability of 5-HT_{1A}autoR to couple effectively to G-proteins and in turn to downstream effectors, and therefore, an inability of the receptor to respond to increased serotonin at the synapse (Riad et al., 2008). This finding naturally leads to exciting directions for research and the possibility of inhibiting the receptor at treatment onset in order to promote treatment efficacy right from the start.

A greater understanding of 5-HT_{1A}R receptor function in the depressed state, as well as of the mode of action of SSRIs on 5-HT_{1A}autoR function might lead to better treatment options in

the future. Toward this goal, the possibility of investigating 5-HT_{1A}autoR internalization with the microPET in rat would represent a remarkable addition to current experimental methods. This approach could be applied in several contexts, including rat models of depression, in which the mode of action of SSRI antidepressants could also be investigated. All available data on the internalization of 5-HT_{1A} receptors have indeed been collected in human volunteers and healthy laboratory animals. However, the mechanisms of action of SSRI antidepressants could be altered in the depressed state. The internalization of 5-HT_{1A}autoR during and after antidepressant treatment could also be studied in relation to behavior to discriminate treatment responders from non-responders in those animal models of depression, and to study the fate of these receptors after cessation of treatment. This could provide insights into mechanisms accounting for the lack of responsiveness to SSRI treatment and persistence of symptoms or recurrence of the disease.

The knowledge acquired from such investigations could then be translated to human studies and eventually lead to early assessment of treatment efficacy in depressed individuals. [^{18}F]MPPF BP_{ND} has already been measured both in epilepsy (Merlet et al, 2004), with decreased binding found in epileptogenic regions, and in Alzheimer's disease, discovering a significant association between BP in hippocampus and symptom severity (Kepe et al, 2006). The measurement of [^{18}F]MPPF BP_{ND} would therefore likely be equally useful in the context of psychopathology such as depression.

ACKNOWLEDGEMENTS

The author was supported financially by the Canadian Institutes for Health Research (CIHR), the Fonds de la Recherche en Santé du Québec (FRSQ) and the graduate program in

neuroscience (GPNS) at McGill. The technical assistance of Antonio Alliaga with the microPET imaging, and the help of Nicolas Aznavour and Paul Gravel in the analysis of the microPET data are gratefully acknowledged. The author is also grateful to Mustapha Riad for his substantial collaboration to the preparation and analysis of the immuno-electron microscopic material demonstrating the internalization of 5-HT_{1A} receptors. She appreciates the help of Dr. Linda Booij and Alexandra Sousa-Pires in accompanying human participants to the PET unit so that she would be free to concurrently run her animal scans. She also thanks Vinod Venugopalan for advice and support during the writing of the manuscript. Finally, she thanks her advising committee members, Dr. Marco Leyton and Dr. Simon Young, as well as her supervisors, Dr. Chawki Benkelfat and Dr. Laurent Descarries, for their guidance and support throughout her Masters, with special thanks to Dr. Descarries for his considerable help in the writing of the manuscript.

REFERENCES

Adell, A., Celada, P., Abellan, M.T., Artigas, F. (2002). Origin and functional role of the extracellular serotonin in the midbrain raphe nucleus. *Brain Res Rev, 39*, 154-180.

Ansorge, M.S., Hen, R., Gingrich, J.A. (2007). Neurodevelopmental origins of depressive disorders. *Curr Opin Pharmacol, 7*, 8-17.

Aznavour, N., Zimmer, L. (2007). [^{18}F]MPPF as a tool for the in vivo imaging of 5-HT_{1A} receptors in animal and human brain. *Neuropharmacology, 52*, 695-707.

Aznavour, N., Rbah, L., Riad, M., Reilhac, A., Costes, N., Descarries, L., Zimmer, L. (2006). A PET imaging study of 5-HT1A receptors in cat brain after acute and chronic fluoxetine treatment. *NeuroImage, 33*, 834-842.

Aznavour, N., Benkelfat, C., Gravel, P., Aliaga, A., Rosa-Neto, P., Bedell, B., Zimmer, L., Descarries, L. (2009). MicroPET imaging of 5-HT_{1A} receptors in rat brain: a test-retest [^{18}F]MPPF study. *Eur J Nucl Med Mol Imaging, 36*, 53-62.

Bailer, U.F., Frank, G.K., Henry, S.E., Price, J.C., Meltzer, C.C., Weissfeld, L., et al. (2005). Altered brain serotonin 5-HT_{1A} receptor binding after recovery from anorexia nervosa measured by positron emission tomography and [carbonyl^{11}C]WAY 100635. *Arch Gen Psychiatry, 62*, 1032-1041.

Barnes, N.M., Sharp, T. (1999). A review of central 5-HT receptors and their function. *Neuropharmacology, 38*, 1083-1152.

Beer, M., Kennett, G.A., Curzon, G. (1990). A single dose of 8-OH-DPAT reduces raphe binding of [^{3}H]8-OH-DPAT and increases the effect of raphe stimulation of 5-HT metabolism. *Eur J Pharmacol, 178*, 179-187.

Blier, P., de Montigny, C. (1987). Modification of 5-HT neuron properties by sustained administration of the 5-HT agonist gepirone: electrophysiological studies in the rat brain. *Synapse, 1*, 470-480.

Blier, P., de Montigny, C. (1994). Current advances and trends in the treatments of depression. *Trends Pharmacol Sci, 15*, 220-226.

Bohmaker, K., Eison, A.S., Yocca, F.D., Meller, E. (1993). Comparative effects of chronic 8-OH-DPAT, gepirone and ipsapirone treatment on the sensitivity of somatodendritic 5-HT1A autoreceptors. *Neuropharmacology, 32*, 527-534.

Booij, L., van der Does, W., Benkelfat, C., Bremner, J.D., Cowen, P.J., Fava, M., et al. (2002). Predictors of mood response to acute tryptophan depletion. A reanalysis. *Neuropsychopharmacology, 27*, 852-861.

Brundtland, G.H. (2001). From the World Health Organization. Mental Health: new understanding, new hope. *JAMA, 286*, 2391.

Caspi, A., Sugden, K., Moffitt, T.E., Taylor, A., Craig, I.W., Harrington, H., et al. (2003). Influence of life stress on depression: Moderation by a polymorphism in the 5-HTT gene. *Science, 301*, 386-389.

Choi, S., Jonak, E., Fernstrom, J.D. (2004). Serotonin reuptake inhibitors do not prevent 5,7-dihydroxytryptamine-induced depletion of serotonin in rat brain. *Brain Res, 1007*, 19-28.

Coccaro, E.F. (1996). Neurotransmitter correlates of impulsive aggression in humans. *Ann N Y Acad Sci, 794*, 82-89.

Coppen, A.J., Eccleston, E.G., Peet, M. (1973). Total and free tryptophan concentration in the plasma of depressive patients. *Lancet, 2*, 60-63.

Corradetti, R., Le Poul, E., Laaris, N., Hamon, M., Lanfumey, L. (1996). Electrophysiological

effects of N-(2-(4-(2-methoxyphenyl)-1-piperazinyl)ethyl)-N-(2-pyridinyl) cyclohexane carboxamide (WAY 100635) on dorsal raphe serotonergic neurons and CA1 hippocampal pyramidal cells in vitro. *J Pharmacol Exp Ther, 278*, 678-688.

Costes, N., Merlet, I., Ostrowsky, K., Faillenot, I., Lavenne, F., Zimmer, L., et al. (2005). A ^{18}F-MPPF PET normative database of 5-HT_{1A} receptor binding in men and women over aging. *J Nucl Med, 46*, 1980-1989.

Cowen, P.J., Parry-Billings, M., Newsholme, E.A. (1989). Decreased plasma tryptophan levels in major depression. *J Affect Disord, 16*, 27-31.

Cryan, J.F., Leonard, B.E. (2000). 5-HT_{1A} and beyond: The role of serotonin and its receptors in the depression and the antidepressant response. *Hum Psychopharmacol, 15*, 113-135.

Cunningham, K.A., Lakoski, J.M. (1990). The interaction of cocaine with serotonin dorsal raphe neurons. Single-unit extracellular recording studies. *Neuropsychopharmacology, 3*, 41-50.

Czachura, J.F., Rasmussen, K. (2000). Effects of acute and chronic administration of fluoxetine on the activity of serotonergic neurons in the dorsal raphe nucleus of the rat. *Naunym Schmied Arch Pharmacol, 362*, 266-275.

Davidson, J.R.T. (2006). Pharmacotherapy of social anxiety disorder: What does the evidence tell us? *J Clin Psychiatry, 67*, 20-26.

Delgado, P.L., Charney, D.S., Price, L.H., Aghajanian, G.K., Landis, H., Heninger, G.R. (1990). Serotonin function and the mechanism of antidepressant action. Reversal of antidepressant-induced remission by rapid depletion of plasma tryptophan. *Arch Gen Psychiatry, 47*, 411-418.

Descarries, L., Watkins, K.C., Garcia, S., Beaudet, A. (1982). The serotonin neurons in nucleus raphe dorsalis of adult rat: a light and electron microscope radioautographic study. *J Comp Neurol, 207*, 239-254.

Dong, J., de Montigny, C., Blier, P. (1997). Effect of acute and repeated versus sustained administration of the 5-HT1A receptor agonist ipsapirone: electrophysiological studies in the rat hippocampus and dorsal raphe. *Naunym Schmied Arch Pharmacol, 356*, 303-311.

Elsinga, P.H., Hendrikse, N.H., Bart, J., van Waarde, A., Vaalburg, W. (2005). Positron emission tomography studies on binding of central nervous system drugs and p-glycoprotein function in the rodent brain. *Mol Imaging Biol, 7*, 37-44.

Fargin, A., Raymond, J.R., Lohse, M.J., Kobilka, B.K., Caron, M.G., Lefkowitz, R.J. (1998). The genomic clone G-21 which resembles a beta-adrenergic receptor sequence encodes the 5-HT1A receptor. *Nature, 335*, 358-360.

Fava, M. (2000). Management of nonresponse and intolerance: switching strategies. *J Clin Psychiatry, 61*, 10-12.

Fuller, R.W. (1994). Uptake inhibitors increase extracellular serotonin concentration measured by brain microdialysis, *Life Sci, 55*, 163-167.

Fuller, R.W. (1995). Serotonin uptake inhibitors: uses in clinical therapy and in laboratory research. *Prog Drug Res, 45*, 167-204.

Gaspar, P., Cases, O., Maroteaux, L. (2003). The developmental role of serotonin: News from mouse molecular genetics. *Nat Rev Neurosci, 4*, 1002-1012.

Grant, J.E., Potenza, M.N. (2004). Impulse control disorders: clinical characteristics and pharmacological management. *Ann Clin Psychiatry, 16*, 27-34.

Gross, C., Zhuang, X., Stark, K., Ramboz, S., Oosting, R., Kirby, L., et al. (2002). Serotonin1A receptor acts during development to establish normal anxiety-like behaviour in the adult. *Nature, 416*, 396-400.

Gunn, R.N., Sargent, P.A., Bench, C.J., Rabiner, E.A., Osman, S., Pike, V.W., et al. (1998). Tracer kinetic modeling of the 5-HT1A receptor ligand [*carbonyl*-^{11}C]WAY-100635 for PET. *NeuroImage, 8*, 426-440.

Hamon, M., Fattacini, C.M., Adrien, J., Gallisot, M.C., Martin, P., Gozlan, H. (1988). Alterations of central serotonin and dopamine turnover in rats treated with ipsapirone and other 5-hydroxytryptamine 1A agonists with potential anxiolytic properties. *J Pharmacol Exp Ther, 246*, 745-752.

Hervás, I., Artigas, F. (1998). Effect of fluoxetine on extracellular 5-hydroxytryptamine in rat brain. Role of 5-HT autoreceptors. *Eur J Pharmacol, 358*, 9-18.

Higley, J.D., Linnoila, M. (1997). Low central nervous system serotonergic activity is traitlike and correlates with impulsive behaviour. *Ann N Y Acad Sci, 836*, 39-56.

Hoffman, E.J., Huang, S.C., Phelps, M.E. (1979). Quantification in positron emission computed tomography: 1. Effect of object size. *J Comput Assist Tomogr, 3*, 299-308.

Hutson, P.H., Sarna, G.S., O'Connell, M.T., Curzon, G. (1989). Hippocampal 5-HT synthesis and release in vivo is decreased by infusion of 8-OH-DPAT into the nucleus raphe dorsalis. *Neurosci Lett, 100*, 276-280.

Innis, R.B., Cunningham, J., Delforge, J., Fujita, M., Gjedde, A., Gunn, R.N., et al. (2007). Consensus nomenclature for the in vivo imaging of reversibly binding radioligands. *J Cereb Blood Flow Metab, 27*, 1533-1539.

Invernizzi, R., Bramante, M., Samanin, R. (1996). Role of 5-HT1A receptors in the effects of acute and chronic fluoxetine on extracellular serotonin in the frontal cortex. *Pharmacol Biochem Behav, 54*, 143-147.

Irons, J. (2005). Fluvoxamine in the treatment of anxiety disorders. *Neuropsychiatr Dis Treat, 1*, 289-299.

Kaye, W. (2008). Neurobiogy of anorexia and bulimia nervosa. *Physiol Behav, 94*, 121-135.

Kaye, W., Frank, G.K., Bailer, U., Henry, S.E. (2005). Neurobiology of anorexia nervosa: Clinical implications of alterations of the function of serotonin and other neuronal systems. *Int J Eat Disord, 37*, S15-S19.

Kennett, G.A., Marcou, M., Dourish, C.T., Curzon, G. (1987). Single administration of 5-HT1A agonists decreases 5-HT1A presynaptic, but not postsynaptic receptor-mediated responses: relationship to antidepressant-like action. *Eur J Pharmacol, 138*, 53-60.

Kepe, B., Barrio, J.R., Huang, S.C., Ercoli, L., Siddarth, P., Shoghi-Jadid, K., et al. (2006). Serotonin 1A receptors in the living brain of Alzheimer's disease patients. *Proc Natl Acad Sci U S A, 103*, 702-207.

Kia, H.K., Miquel, M.C., Brisorgueil, M.J., Daval, G., Riad, M., El Mestikawy, S., et al. (1996). Immunocytochemical localization of serotonin1A receptors in the rat central nervous system. *J Comp Neurol, 365*, 289-305.

Knoess, C., Siegel, S., Smith, A., Newport, D., Richerzhagen, N., Winkeler, A., et al. (2003). Performance evaluation of the microPET R4 PET scanner for rodents. *Eur J Nucl Med Mol Imaging, 30*, 737-747.

Kreiss, D.S., Lucki, I. (1995). Effects of acute and repeated administration of antidepressant drugs on extracellular levels of 5-hydroxytryptamine measured in vivo. *J Pharmacol Exp Ther, 274*, 866-876.

Lanfumey, L., Hamon, M. (2004). 5-HT1 receptors. *Curr Drug Targets CNS Neurol Disord, 3,* 1-10.

Lanfumey, L., Haj-Dahmane, S., Hamon, M., (1993). Further assessment of the antagonist properties of the novel and selective 50HT1A receptor ligands (+)-WAY 100 135 and SDZ 216-525. *Eur J Pharmacol, 249*, 25-35.

Le Bars, D., Lemaire, C., Ginovart, N., Plenevaux, A., Aerts, J., Brihaye, C., et al. (1998). High-yield radiosynthesis and preliminary in vivo evaluation of p[^{18}F]MPPF, a fluoro analog of WAY-100635. *Nucl Med Bio, 25*, 343-350.

Le Poul, E., Laaris, N., Hamon, M., Lanfumey, L. (1997). Fluoxetine-induced desensitization of somatodendritic 5-HT1A autoreceptors is independent of glucocorticoid(s). *Synapse, 27*, 303-312.

Lemonde, S., Du, L., Bakish, D., Hrdina, P., Albert, P.R. (2004). Association of the C(-1019)G 5-HT1A functional promoter polymorphism with antidepressant response. *Int J Neuropsychopharmacol, 7*, 501-506.

Lesch, K.P., Bengel, D., Heils, A., Sabol, S.Z., Greenberg, B.D., Petri, S., et al. (1996). Association of anxiety-related traits with a polymorphism in the serotonin transporter gene regulatory region. *Science, 274*, 1527-1531.

Malagié, I., Trillat, A.C., Jacquot, C., Gardier, A.M. (1995). Effects of acute fluoxetine on extracellular serotonin levels in the raphe: an in vivo microdialysis study. *Eur J Pharmacol, 286*, 213-217.

Marchese, A., Paing, M.M., Temple, B.R.S., Trejo, J. (2008). G protein-coupled receptor sorting to endosomes and lysosomes. *Annu Rev Pharmacol Toxicol, 48*, 601-629.

Martin, L.P., Jackson, D.M., Wallsten, C., Waszczak, B.L. (1999). Electrophysiological comparison of 5-hydroxytryptamine1A receptor antagonists on dorsal raphe cell firing. *J Pharmacol Exp Ther, 288*, 820-826.

Merlet, I., Ostrowsky, K., Costes, N., Ryvlin, P., Isnard, J., Faillenot, I., et al. (2004). 5-HT_{1A} receptor binding and intracerebral activity in temporal lobe epilepsy: an [^{18}F]MPPF-PET study. *Brain, 127*, 900-913.

Meyers, S. (2000). Use of neurotransmitter precursors for treatment of depression. *Altern Med Rev, 5*, 64-71.

Millan, M.J. (2006). Multi-target strategies for the improved treatment of depressive states: Conceptual foundations and neuronal substrates, drug discovery and therapeutic applications. *Pharmacol Therap, 110*, 135-370.

Millet, P., Moulin, M., Bartoli, A., Del Guerra, A., Ginovart, N., Lemoucheux, L., et al. (2008). *In vivo* quantification of 5-HT_{1A}-[^{18}F]MPPF interactions in rats using the YAP-(S)PET scanner and a β-microproble. *NeuroImage, 41*, 823-834.

Moeller, F.G., Barratt, E.S., Dougherty, D.M., Schmitz, J.M., Swann, A.C. (2001). Psychiatric aspects of impulsivity. *Am J Psychiatry, 158,* 1783-1793.

Moore, C.A., Milano, S.K., Benovic, J.L. (2007). Regulation of receptor trafficking by GRKs and arrestins. *Annu Rev Physiol, 69*, 451-482.

Moulin-Sallanon, M., Charnay, Y., Ginovart, N., Perret, P., Lanfumey, L., Hamon, M., et al. (2009). Acute and chronic effects of citalopram on 5-HT1A receptor–labeling by [^{18}F]MPPF and coupling–to receptors-G proteins. *Synapse, 63*, 106-116.

Mundey, M. K., Fletcher, A., Marsden, C.A. (1994). Effect of the putative 5-HT1A antagonist WAY-100635 on 5-HT neuronal firing in the guinea-pig dorsal raphe nucleus. *Neuropharmacology, 33*, 61-66.

Nelson, R.J., Trainor, B.C. (2007). Neural mechanisms of aggression. *Nat Rev Neurosci, 8*, 536-546.

Nemeroff, C.B., Owens, M.J. (2002). Treatment of mood disorders. *Nat Neurosci, 5*, 1068-1070.

Neumeister, A., Nugent, A.C., Waldeck, T., Geraci, M., Schwarz, M., Bonne, O., et al. (2004). Neuronal and behavioral responses to tryptophan depletion in unmedicated patients with remitted major depressive disorder and controls. *Arch Gen Psychiatry, 61*, 765-773.

Neumeister A, Hu, X.Z., Luckenbaugh, D.A., Schwartz, M., Nugent, A.C., Bonne, O., et al. (2006). Differential effects of 5-HTTLPR genotypes on the behavioral and neural responses to tryptophan depletion in patients with major depression and controls. *Arch Gen Psychiatry, 63*, 978-986.

Nichols, D.E., Nichols, C.D. (2008). Serotonin Receptors. *Chem Rev, 108*, 1614-1641.

Nutt, D.J., Stein, D.J. (2006). Understanding the neurobiology of comorbidity in anxiety disorders. *CNS Spectr, 11*, 13-20.

Parsey, R.V., Arango, V., Olvet, D.M., Oquendo, M.A., van Heertum, R.L., John Mann, J. (2005). Regional heterogeneity of 5-HT1A receptors in human cerebellum as assessed by positron emission tomography. *J Cereb Blood Flow Metab, 25*, 7, 785-793.

Passchier, J., van Waarde, A. (2001). Visualisation of serotonin-1A (5-HT_{1A}) receptors in the central nervous system. *Eur J Nucl Med, 28,* 113-129.

Passchier, J., van Waarde, A., Pieterman, R.M., Elsinga, P.H., Pruim, J., Hendrikse, H.N., et al. (2000a). Quantitative imaging of 5-HT(1A) receptor binding in healthy volunteers with [(18)F]p-MPPF. *Nucl Med Biol, 27*, 473-476.

Passchier, J., van Waarde, A., Pieterman, R.M., Elsinga, P.H., Pruim, J., Hendrikse, H.N., et al. (2000b). In vivo delineation of 5-HT_{1A} receptors in human brain with [^{18}F]MPPF. *J Nucl Med, 41,* 1830-1835.

Pattij, T., Vanderschuren, L.J.M.J. (2008). The neuropharmacology of impulsive behaviour. *Trends Pharmacol Sci, 29*, 192-199.

Pazos, A., Palacios, J.M. (1985). Quantitative autoradiographic mapping of serotonin receptors in the rat brain. I. Serotonin-1 receptors. *Brain Res, 346*, 205-230.

Piñeyro, G., Blier, P. (1999). Autoregulation of serotonin neurons: role in antidepressant drug action. *Pharmacol Rev, 51*, 533-591.

Plénevaux, A., Weissman, D., Aerts, J., Lemaire, C., Brihaye, C., Degueldre, C., et al. (2000). Tissue distribution, autoradiography, and metabolism of 4-(2'-methoxyphenyl)-1-[2'-[N-2"-pyridinyl)-*p*-[(^{18})F]fluorobenzamido]ethyl]piperazine (*p*-[^{18}F]MPPF), a new serotonin 5-HT_{1A} antagonist for positron emission tomography: an in vivo study in rats. *J Neurochem, 75*, 803-811.

Ramboz, S., Oosting, R., Amara, D.A., Kung, H.F., Blier, P., Mendelsohn, M., et al. (1998). Serotonin 1A knockout: an animal model of anxiety-related disorder. *Proc Natl Acad Sci U S A, 95*, 14476-14481.

Raymond, J.R., Mukhin, Y.V., Gettys, T.W., Garnovskaya, M.N. (1999). The recombinant 5-HT1A receptor: G protein coupling and signaling pathways. *Brit J Pharmacol, 127*, 1751-1764.

Riad, M., Garcia, S., Watkins, K.C., Jodoin, N., Doucet, E., Langlois, X., et al. (2000). Somatodendritic localization of 5-HT_{1A} and preterminal axonal localization of 5-HT_{1B} serotonin receptors in adult rat brain. *J Comp Neurol, 417*, 181-194.

Riad, M., Watkins, K.C., Doucet, E., Hamon, M., Descarries, L. (2001). Agonist-induced internalisation of serotonin-1A receptors in the dorsal raphe nucleus (autoreceptors) but not hippocampus (heteroreceptors). *J Neurosci, 21*, 8378-8386.

Riad, M., Zimmer, L., Rbah, L., Watkins, K.C., Hamon, M., Descarries, L. (2004). Acute treatment with the antidepressant fluoxetine internalizes 5-HT_{1A} autoreceptors and reduces the in vivo binding of the PET radioligand [^{18}F]MPPF in the nucleus raphe dorsalis of rat. *J Neurosci, 24*, 5420-5426.

Riad, M., Rbah, L., Verdurand, M., Aznavour, N., Zimmer, L., Descarries, L. (2008). Unchanged density of 5-HT1A autoreceptors on the plasma membrane of nucleus raphe dorsalis neurons in rats chronically treated with fluoxetine. *Neuroscience, 151*, 692-700.

Rigdon, G.C., Wang, CM., (1991). Serotonin uptake blockers inhibit the firing of presumed serotonergic dorsal raphe neurons in vitro. *Drug Dev Res, 22*, 135-140.

Rosenbaum, D.M., Rasmussen, S.G.F. (2009). The structure and function of G-protein-coupled receptors. *Nature, 459*(7245), 356-363.

Rothe, C., Gutknecht, L., Freitag, C., Tauber, R., Mossner, R., Franke, P., et al. (2004). Association of a functional -1019C>G 5-HT1A receptor gene polymorphism with panic disorder with agoraphobia. *Int J Neuropsychopharmacol, 7*, 189-192.

Rutter, J.J., Auerbach, S.B. (1993). Acute uptake inhibition increases extracellular serotonin in the rat forebrain. *J Pharmacol Exp Ther, 265*, 1319-1324.

Rutter, J.J., Gundlah, C., Auerbach, S.B. (1995). Systemic uptake inhibition decreases serotonin release via somatodendritic autoreceptor activation, *Synapse, 20*, 225-233.

Seth, P., Gajendiran, M., Ganguly, D.K. (1997). Desensitization of spinal 5-HT1A receptors to 8-OH-DPAT: an in vivo spinal reflex study. *NeuroReport, 8*, 2489-2493.

Sharp, T., Branwell, S.R., Grahame-Smith, D.G. (1989). 5-HT1 agonists reduce 5-hydroxytryptamine release in rat hippocampus in vivo as determined by brain microdialysis. *Br J Pharmacol, 96*, 283-290.

Sharp, T., Umbers, V., Hjorth, S., (1996). The role of 5-HT1A autoreceptors and alpha 1-adrenoceptors in the inhibition of 5-HT release—II NAN-190 and SDZ 216-525. *Neuropharmacology, 35*, 735-741.

Shively, C.A., Friedman, D.P., Gage, H.D., Bounds, M.C., Brown-Proctor, C., Blair, J.B., et al. (2006). Behavioral depression and positron emission tomography-determined serotonin 1A receptor binding potential in cynomolgus monkeys. *Arch Gen Psychiatry, 63*, 396-403.

Sibon, I., Benkelfat, C., Gravel, P., Aznavour, N., Costes, N., Mzengeza, S., et al. (2008). Decreased [^{18}F]MPPF binding potential in the dorsal raphe nucleus after a single oral dose of fluoxetine: A PET study in healthy volunteers. *Biol Psychiatry, 63*, 1135-1140.

Sprouse, J.S., Aghajanian, G.K. (1987). Electrophyiological responses of serotonergic dorsal raphe neurons to 5-HT1A and 5-HT1B agonists. *Synapse, 1*, 3-9.

Srinivas, S.M., Dhurairaj, T., Basu, S., Bural, G., Surti, S., Alavi, A. (2009). A recovery coefficient method for partial volume correction of PET images. *Ann Nucl Med, 23*, 341-348.

Steinbusch, H.W.M. (1981). Distribution of serotonin immunoreactivity in the central nervous system of the rat. Cell bodies and terminals. *Neuroscience, 6*, 557-618.

Strobel, A., Gutknecht, L., Rothe, C., Reif, A., Mossner, R., Zeng, Y., et al. (2003). Allelic variation in 5-HT1A receptor expression is associated with anxiety- and depression-related personality traits. *J Neural Transm, 110*, 1445-1453.

Sullivan, G.M., Ogden, R.T., Oquendo, M.A, Dileep Kumar, J.S., Simpson, N., Huang, Y.Y., et al. (2009). Positron emission tomography quantification of serotonin-1A receptor binding in medication-free bipolar depression. *Biol Psychiatry, 66*, 223-230.

Tiihonen, J., Keshi-Rahkonen, A., Lopponen, M., Muhonen, M., Kajander, J., Allonen, T., et al. (2004). Brain serotonin 1A receptor binding in bulimia nervosa. *Biol Psychiatry, 55*, 871-873.

Toth, M. (2003). 5-HT1A receptor knockout mouse as a genetic model of anxiety. *Eur J Pharmacol, 463*, 177-184.

van Praag, H.M., Korf, J., Dols, L.C., Schut, T. (1972). A pilot study of the predictive value of the probenecid test in application of 5-hydroxytryptophan as antidepressant. *Psychopharmacologia, 25*, 14-21.

Whitaker-Azmitia, P.M. (2001). Serotonin and brain development: Role in human developmental diseases. *Brain Res Bull, 56*, 479-485.

Wolfe, B.L., Trejo, J. (2007). Clathrin-dependent mechanisms of G protein-coupled receptor endocytosis. *Traffic, 8*, 462-470.

Wrase, J., Reimold, M., Puls, I., Kienast, T., Heinz, A. (2006). Serotonergic dysfunction: Brain imaging and behavioral correlates. *Cogn Affect Behav Neurosci, 6*, 53-61.

Zhuang, Z.P., Kung, M.P., Kung, H.F. (1994). Synthesis and evaluation of 4-(2'-methoxyphenyl)-l-[2'-[N-(2"pyridinyl)-p-iodobenzamido]ethyl]piperazine (p-MPPI): a new iodinated 5-HT_{1A} ligand. *J Med Chem, 37*, 1406-1407.

Zimmer, L., Riad, M., Rbah, L., Belkacem-Kahlouli, A., Le Bars, D., Renaud, B., Descarries, L. (2004). Toward brain imaging of serotonin 5-HT_{1A} autoreceptor internalization. *NeuroImage, 22*, 1421-1426.

Figure 1

MicroPET procedure time line

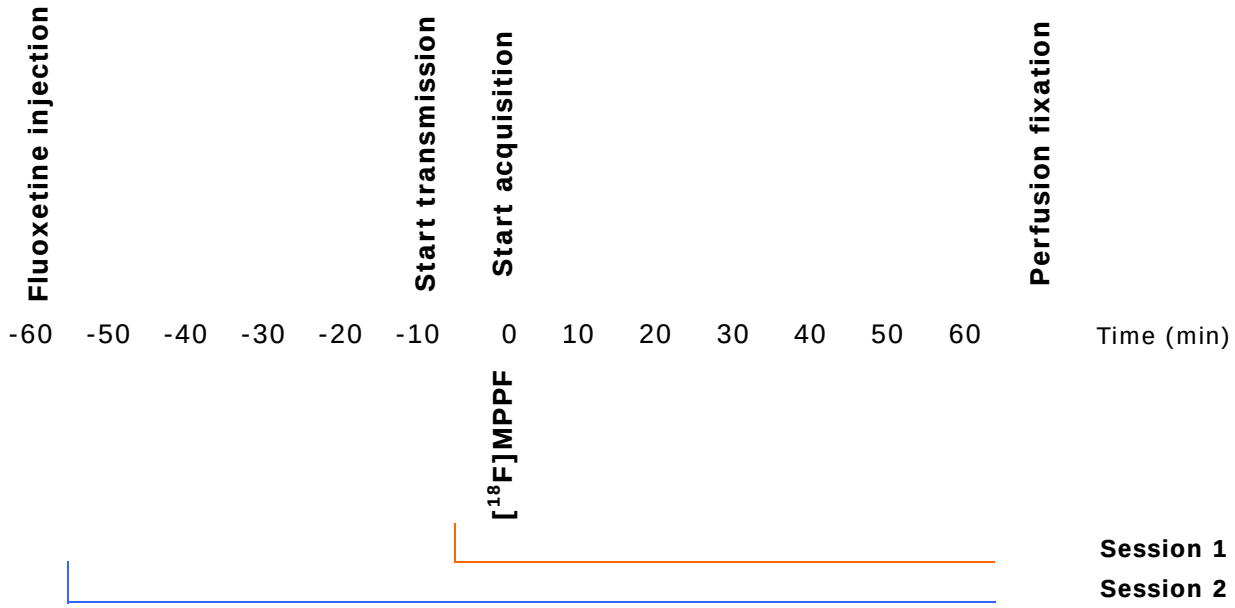

Session 1: Baseline condition. All 10 rats underwent a 10-minute transmission scan followed by a bolus injection with 37 Mbq (1 mCi) in 0.1 ml of [^{18}F]MPPF and a dynamic acquisition of 60 minutes divided into 27 frames.

Session 2: Fluoxetine treatment, 7 or 14 days after baseline. All 10 rats underwent a second scan one hour following the administration of fluoxetine. Then, a subset of 3 rats underwent fixation by perfusion through the aortic arch immediately following the end of scanning and were processed for immuno-electron microscopy.

Table 1

[^{18}F]MPPF BP_{ND} in rat brain at baseline and after acute fluoxetine administration

Region	Untreated	Fluoxetine	% change	t-test	*p*
Medial prefrontal cortex	1.1 ± 0.10	1.1 ± 0.07	-1.24	0.09	0.93
Septum	1.2 ± 0.11	1.2 ± 0.08	-3.15	0.25	0.81
Paraventricular hypothalamus	0.5 ± 0.07	0.5 ± 0.08	15.25	-0.59	0.57
Basolateral amygdala	0.8 ± 0.07	0.9 ± 0.05	6.30	-0.75	0.47
Hippocampus	1.1 ± 0.10	1.2 ± 0.08	8.61	-1.00	0.34
Entorhinal cortex	1.0 ± 0.14	1.0 ± 0.10	8.55	-0.66	0.52
Raphe nuclei	0.5 ± 0.09	0.5 ± 0.07	5.61	-0.25	0.81
Raphe obscurus	0.4 ± 0.09	0.4 ± 0.06	4.12	-0.13	0.90
Cerebellum	0.1 ± 0.01	0.1 ± 0.03	52.98	-1.45	0.18

Means ± SEM of [^{18}F]MPPF BP_{ND} (binding potential) in 10 rats were measured for several regions of interest including the raphe nuclei and areas of projection using the SRTM model with cerebellum white matter as region of reference, as described in Materials and Methods. % change refers to the change between fluoxetine and placebo conditions and was calculated using the following formula: BP (Untreated) – BP (Fluoxetine) / BP (Fluoxetine) X 100. A positive value signifies a decrease in BP following fluoxetine treatment, compared to the untreated condition, and a negative value indicates an increase following fluoxetine treatment.

Figure 2

[^{18}F]MPPF binding in the raphe nuclei at baseline and following acute fluoxetine administration

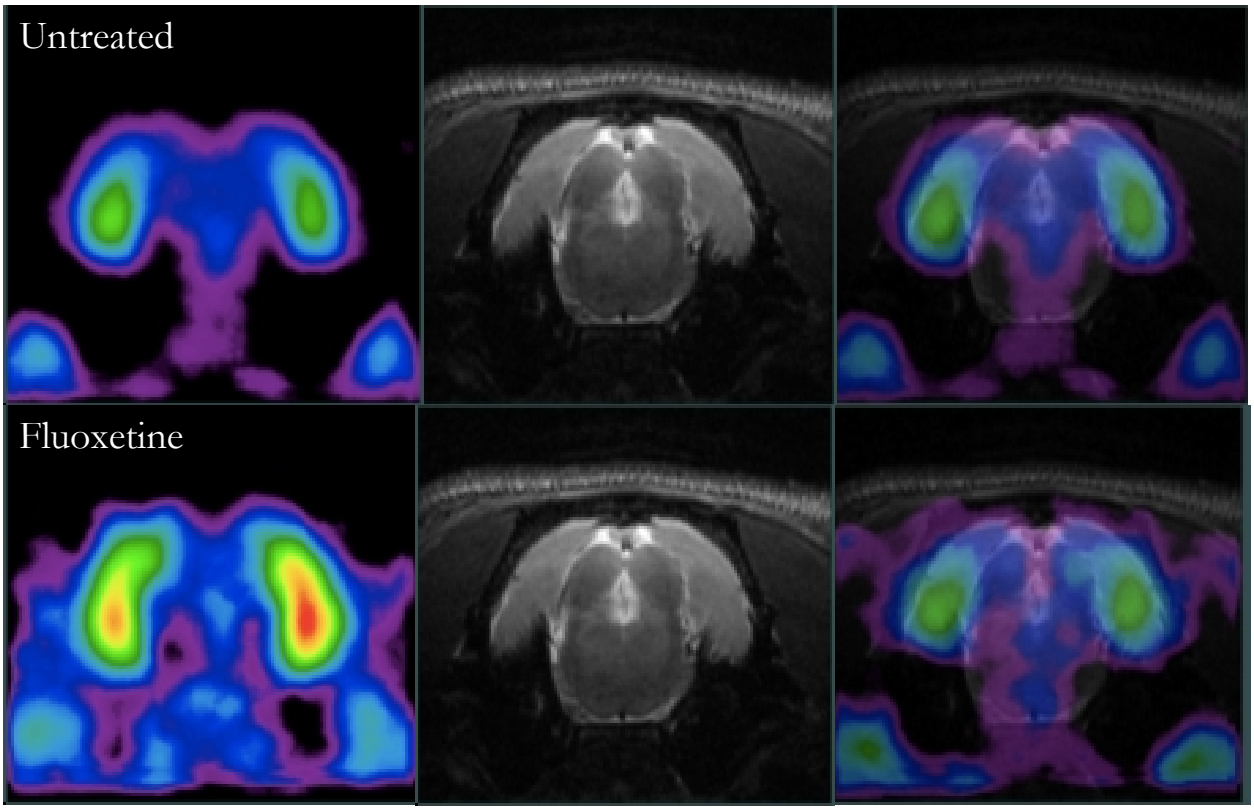

Pseudo-color visualization of [^{18}F]MPPF in raphe nuclei using PET (left), MRI views (middle) and fusion of both types of images (right) at rest (top) and following acute fluoxetine administration (bottom). PET images represent the average BP_{ND} in raphe nuclei across all 10 rats and the MRI is of one male Sprague-Dawley rat, as described in materials and methods.

Figure 3

[^{18}F]MPPF binding in hippocampus at baseline and following acute fluoxetine administration

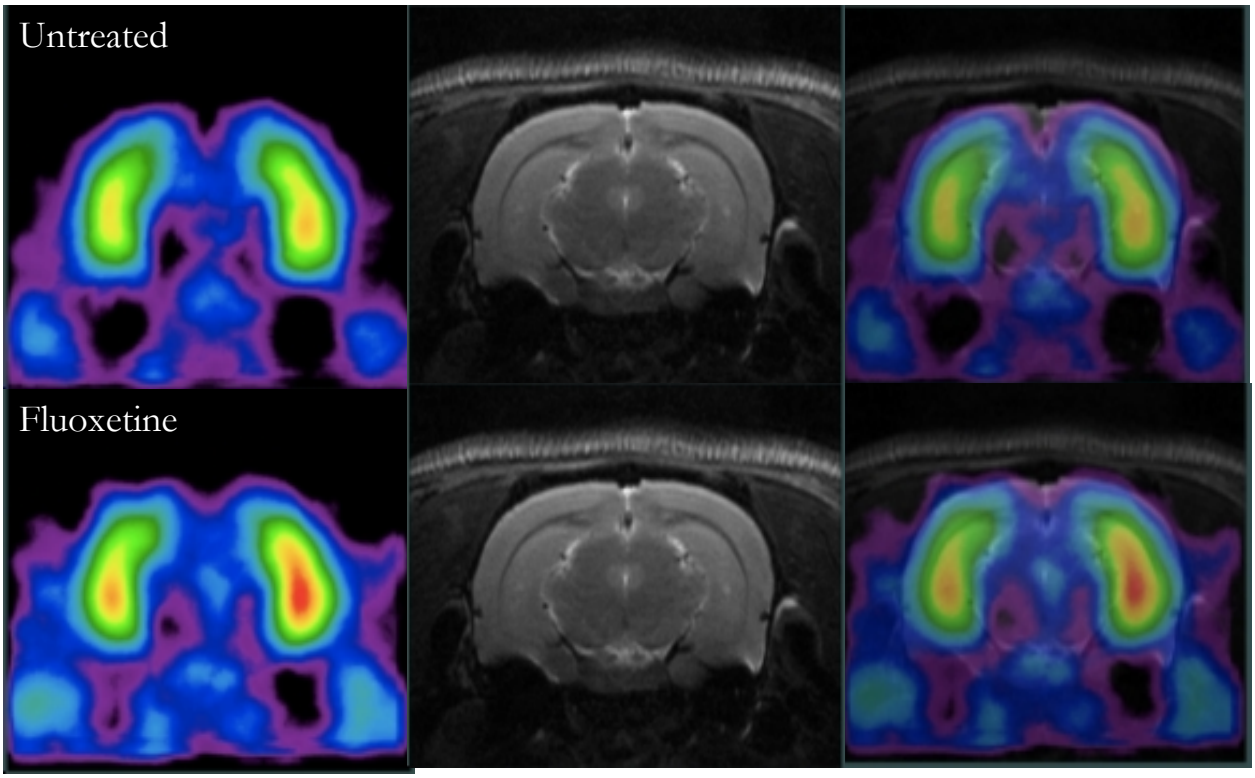

Pseudo-color visualization of [^{18}F]MPPF in HIPP using PET (left), MRI views (middle) and fusion of both types of images (right) at rest (top) and following acute fluoxetine administration (bottom). PET images represent the average BP_{ND} in HIPP across all 10 rats and the MRI is of one male Sprague-Dawley rat, as described in materials and methods.

Figure 4

[^{18}F]MPPF BP_{ND} values at baseline and following acute fluoxetine administration

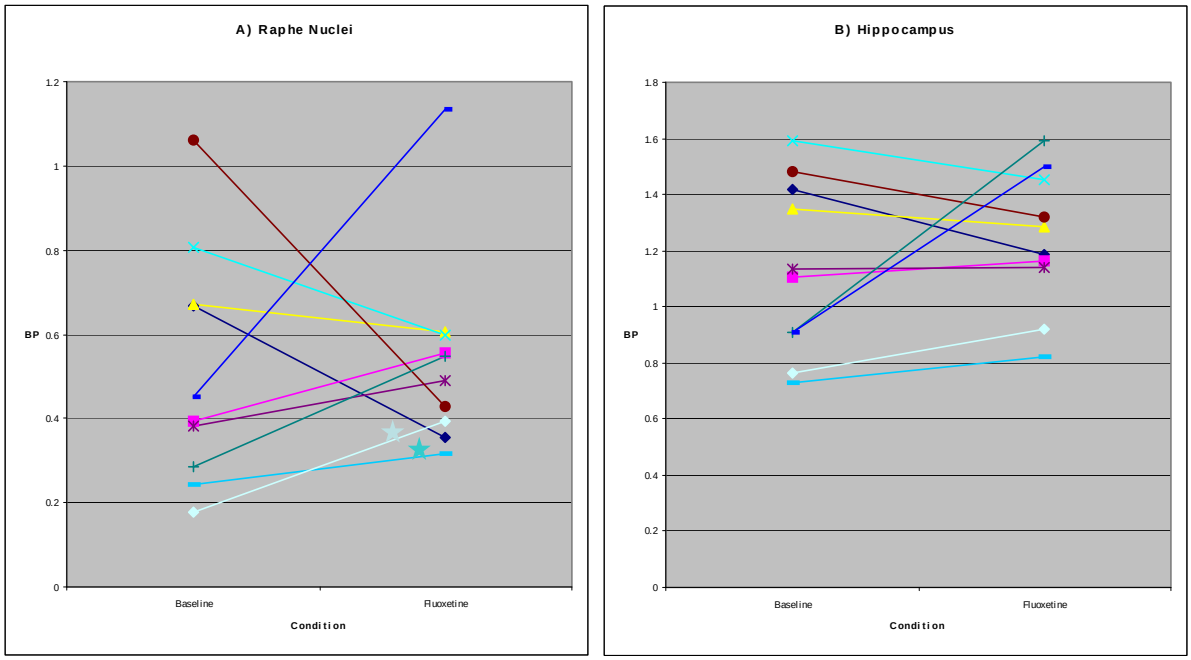

Individual BP_{ND} values from 10 rats in the a) raphe nuclei and b) hippocampus. The DRN of the two rats identified by a star in a) were also examined by 5-HT_{1A}R immuno-electron microscopy. In both regions of interest but especially in the raphe nuclei, data show a lack of consistency in both direction and amplitude of change in [^{18}F]MPPF BP_{ND} following acute fluoxetine administration, compared to baseline (untreated condition).

Figure 5

Immunogold labeling of 5-HT_{1A}autoR in dendrites of rat DRN

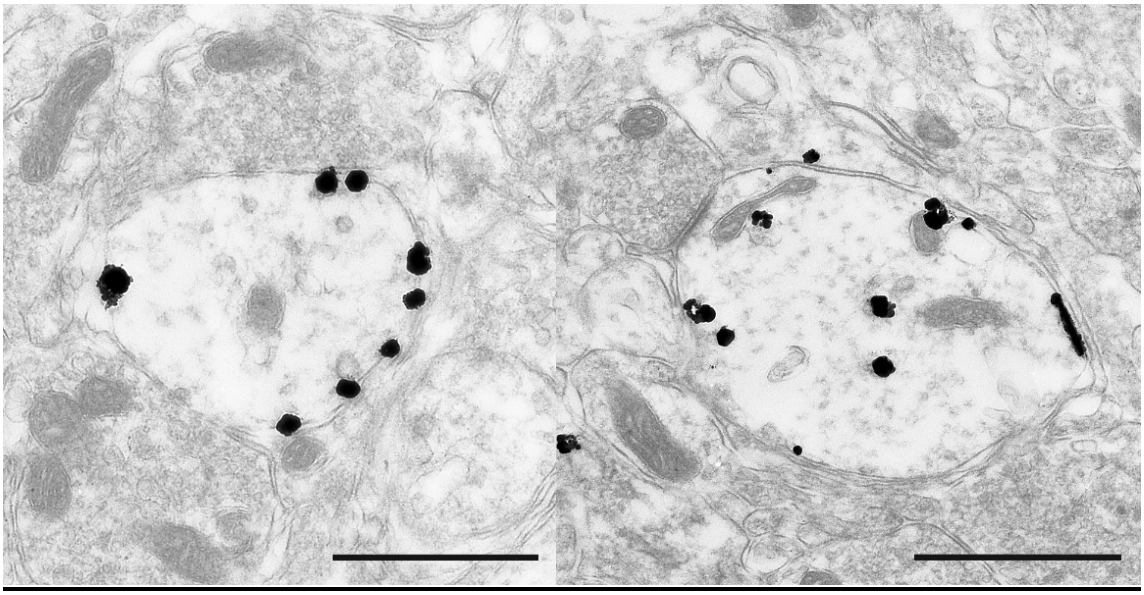

a) untreated b) fluoxetine

Silver-intensified immunogold labeling of 5-HT_{1A}Rs in dendrites from DRN of rats a) which were untreated, and b) 1 hr following acute fluoxetine administration. Note the exclusive localization of receptors to the plasma membrane in untreated animals, and the presence of receptors both at the plasma membrane and within the cytoplasm following fluoxetine administration. Scale bar: 1 μm. Magnification: 17,000X.

Table 2

Density of 5-HT_{1A}autoR immunolabeling in DRN dendrites

Experiment #	Compartment	Control	Fluoxetine
Exp. # 1	Plasmalemma	26.48 (100%)	16.97 (64%)
	Cytoplasm	0.26	0.79
Exp. # 2	Plasmalemma	30.15 (100%)	19.49 (65%)
	Cytoplasm	0.27	0.82
Exp. # 3	Plasmalemma	34.12 (100%)	23.47 (69%)
	Cytoplasm	0.37	1.13

Individual data from untreated and fluoxetine-treated rats. Average number of silver-intensified immunogold particles per surface unit (μm^2) of plasmalemmal and cytoplasmic compartments of DRN dendrites, as explained in Materials and Methods. The fluoxetine-treated rats in Exp. # 1 and 2 are those designated by a star in Fig. 4A. The fluoxetine-treated rat in Exp. # 3 died after 40 min of scanning and was not included in the BP measurements. In order to normalize the data, control (untreated) values of the plasmalemmal compartment were set at 100%, as indicated in brackets. The average number of silver-intensified immunogold particles per surface unit of fluoxetine-treated rats were multiplied by 100 and divided by the average number of particles of untreated rats for each experiment pair. By then subtracting these values from 100, we obtained the corresponding % decrease in average number of particles for each experiment.